Colorimetric derivatization of ambient ammonia (NH$_3$) for detection by long-path absorption photometry

Shasha Tian[1,2], **Kexin Zu**[1,2], **Huabin Dong**[1,2], **Limin Zeng**[1,2], **Keding Lu**[1,2], **and Qi Chen**[1]

[1]State Key Joint Laboratory of Environmental Simulation and Pollution Control, College of Environmental Sciences and Engineering, Peking University, Beijing, 100871, China
[2]International Joint Laboratory of Regional Pollution Control (IJRC), Peking University, Beijing, 100871, China

Correspondence: Huabin Dong (hbdong@pku.edu.cn)

Abstract. In the last few decades, various techniques, including spectroscopic, mass spectrometric, chemiluminescence and wet chemical methods, have been developed and applied for the detection of gaseous ammonia (NH$_3$). We developed an online NH$_3$ monitoring system – salicylic acid derivatization reaction and long-path absorption photometer (SAC-LOPAP) – based on a selective colorimetric reaction to form a highly absorbing reaction product and a LOPAP, which could run stably for a long time and be applied to the continuous online measurement of low concentrations of ambient NH$_3$ by optimizing the reaction conditions, adding a constant-temperature module and liquid flow controller. The detection limit reached with this instrument was 40.5 parts per trillion (ppt) with a stripping liquid flow rate of 0.49 mL min^{-1} and a gas sample flow rate of 0.70 L min^{-1}. An inter-comparison of our system with a commercial Picarro G2103 analyzer (Picarro, USA) in Beijing was presented, and the results showed that the two instruments had a good correlation with a slope of 1.00 and an R^2 of 0.96, indicating that the SAC-LOPAP instrument involved in this study could be used for the accurate measurement of NH$_3$.

1   Introduction

Gaseous ammonia (NH$_3$) widely exists in the atmosphere and plays an important role in many atmospheric chemical reactions (Swati and Hait, 2018; Klimczyk et al., 2021; Wang et al., 2018). As the most abundant alkaline gas in the atmosphere, NH$_3$ easily forms ammonium ions (NH$_4^+$) with water and reacts with acidic species to form secondary inorganic particles (Ianniello et al., 2011; Ni et al., 2000). These secondary particles are considered a major source of fine particulate matter (PM), which is harmful to climate, visibility and human health (Bu et al., 2021; Gao et al., 2021). Furthermore, recent studies have shown that NH$_3$ is necessary to control fine particulate pollution (Wen et al., 2018; Wang et al., 2013). Due to those problems, the inventory of NH$_3$ emissions and the concentration in urban air has been highly evaluated. Agriculture, including animal feedlot operations, is considered the largest emission source of NH$_3$ with 80.6 % of the global anthropogenic emissions followed by 11 % from biomass burning and 8.3 % from the energy sector, including industries and traffic (Behera et al., 2013). Experts estimate that global annual emissions of NH$_3$ will increase from 65 in 2008 to 135 Tg N yr^{-1} in 2100 (Fowler et al., 2015). However, ambient measurement of NH$_3$ concentrations is difficult due to several factors: ambient levels vary widely from 5 parts per trillion by volume (pptv)) to 500 ppbv (Janson et al., 2010; Krupa, 2003; Sutton et al., 1995). Ammonia exists in gaseous, particulate and liquid phases, which further complicates the measurement (Warneck, 1988). In addition, NH$_3$ is "sticky" and interacts with surfaces of materials, resulting in slow inlet response times (Yokelson et al., 2003). Finally, the temperature difference between the indoor and outdoor environments and the humidity difference between the inside and outside of the instrument will reduce the accuracy of measurement and calibration. It is therefore essential to accurately measure ambient NH$_3$ to better quantify concentration and concentration changes and hence to evaluate the impacts of NH$_3$.

In recent years, researchers have developed techniques and methods for detecting NH_3 in the atmosphere, which include spectroscopic, mass spectrometric, chemiluminescence and wet chemical methods (von Bobrutzki et al., 2009). Spectroscopic methods, such as cavity-enhanced absorption spectroscopy (CEAS) (Gong et al., 2017; Berden et al., 2000) and cavity ring-down spectroscopy (CRDS) (Martin et al., 2016; Qu et al., 2012), can greatly improve spectral absorption's effective optical path length by using the optical cavity structure. However, the "stickiness" of NH_3 will affect the background, detection efficiency and detection response time of the instrument (Whitehead et al., 2008; Yokelson et al., 2003). Utilizing a quantum cascade laser (QCL) or a distributed-feedback (DFB) laser in a near-infrared band as the light source can achieve a low detection limit of 0.018 ppb (Whitehead et al., 2008; McManus et al., 2002; von Bobrutzki et al., 2009), realizing the measurement of low concentrations of NH_3 in ambient air. Mass spectrography analyzers provide highly sensitive techniques but may be less specific and can be affected by competing ion chemistries. The chemical ionization mass spectrometer (CIMS) technique is based on an ion–molecule reaction to selectively ionize and detect trace NH_3 in the atmosphere, and it features a fast response and in situ measurement (Benson et al., 2010; Nowak et al., 2007; Yu and Lee, 2012). It has the advantages of a small volume and wide measurement range, but its detection limit is very high (Ajay and Beniwal, 2019). Chemiluminescence is an indirect method to measure ammonia. Two catalytic converters of different characteristics catalyze NO_x and NO amine into NO. The NH_3 mixing ratio is calculated by the difference between NO_x and NO amine. This method can realize the simultaneous measurement of NH_3, NO and NO_2, but the measurement results are affected by the conversion efficiency (Sharma et al., 2010, 2012). Wet-chemistry methods convert gas-phase NH_3 to aqueous NH_3 (NH_4^+) for online analysis by means of online ion chromatography with a detection limit of $0.05\,\mu g\,m^{-3}$ (0.72 ppb at $25\,°C$) (Khlystov et al., 1995; Dong et al., 2012; Makkonen et al., 2012). A field inter-comparison of NH_3 measurement techniques found that wet-chemistry instruments showed better long-term stability and agreement than other analyzers (von Bobrutzki et al., 2009), which was due to the wet chemical trapping method and standard calibration solutions; humidity did not affect the measurement, and the standard solution was more stable than standard gases. However, these instruments failed to capture the peak because of lower time resolution. Based on a selective colorimetric reaction, using aqueous scrubbing in a glass frit impactor to collect NH_3 (and ammonium) to form a highly absorbing reaction product (Bianchi et al., 2012; Bae et al., 2007) has been used for decades for routine derivatization and colorimetric analysis of NH_4^+ in a wide variety of environmental samples (e.g., soils, environmental waters), which has also been reported by other scholars. In those studies the product was detected by a long-path absorption photometer (LOPAP), in which the absorbance of the solution is amplified in the long-path module to reach a lower detection limit (Heland et al., 2001).

In this study, we provide an online NH_3 monitoring system based on wet-chemistry stripping of atmospheric NH_3, followed by the formation of a highly light-absorbing indophenol after a salicylic acid derivatization reaction to produce the colored reaction product detected with a LOPAP. According to the Beer–Lambert law, the sensitivity of spectrophotometry can be enhanced by increasing the optical path length. This sensitive analytical method has already been successfully applied in different colorimetric detection studies (Yao et al., 1998; Heland et al., 2001; Callahan et al., 2002). In analogy to the original long-path absorption photometer (LOPAP), which was developed for HONO measurements (Kleffmann et al., 2002), we call this monitoring system the salicylic acid derivatization reaction and long-path absorption photometer (SAC-LOPAP). It features several improvements over versions previously reported by other groups: one is the optimization of reaction conditions, and another modification is the use of a constant-temperature module and flow control system. Secondly, we will present measurements demonstrating our new system in urban environments in Peking University, with low concentrations, good stability and a low detection limit.

2 SAC-LOPAP instrument

2.1 Measurement principle

Our instrument is designed to measure NH_3 in a low-concentration environment (under 20 ppb) with good stability, a low detection limit (less than 60 ppt) and small size. There is a brief introduction to the principle of the instrument. The measurement of NH_3 in the SAC-LOPAP instrument is achieved by the selective colorimetric reaction to form a highly absorbing reaction product and conduct absorption spectrophotometry. Samples containing dissolved ammonia and ammonium react with a phenolic compound and a chlorine-donating reagent to form indophenol blue during the reaction, with the strongest absorption at a wavelength of 665 nm (Krom, 1980; Searle, 1984). The reaction mechanism of the chromogenic reactions is shown in Eqs. (1)–(4). Furthermore, to measure the absorbance of the sample, we used a LOPAP based on liquid waveguide capillary cell (LWCC) technology to obtain a better detection limit, better continuity and better stability (Heland et al., 2001). TS1

$$NH_3 + HOCl \rightleftharpoons NH_2Cl + H_2O \qquad (1)$$

$$\qquad (2)$$

$$\qquad (3)$$

$$\qquad (4)$$
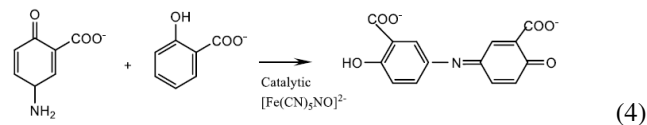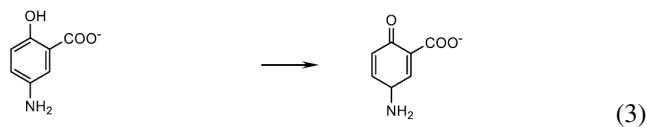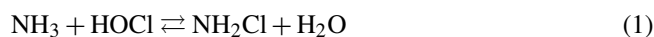
2.2 Experiment setup

We designed our system to consist of four modules: the sampling module, the reacting module, the detecting module and the control module (Fig. 1). The key component of the sampling module is a glass coil reactor, which is an open glass tube (inner diameter 1.5 mm, 75 cm long) coiled for 12 turns. At the beginning of this coil, there is a flow manifold to mix the ambient airflow and the stripping solutions. The air is pumped into the stripping coil under the action of a vacuum diaphragm air pump and a gas flowmeter (Horiba, China) (Chen et al., 2004). To protect the gas flowmeter and the air pump, a security bottle is installed in front of the gas flowmeter to prevent the inflow of liquid. At the same time, the stripping solution, regulated by the liquid flow control system, is injected into the stripping coil to capture NH_3 in the air and form a mixture of ammonium–salicylic acid. To achieve higher absorption efficiency, circulating cooling water with a temperature of 10–15 °C is provided outside the stripping coil. The center part of the reacting module is a reaction coil and a debubbler. The liquid sample is mixed with the alkaline derivatization solution, and a derivatization reaction to produce the colored reaction product reaction occurs in the heated reaction coil. The reaction coil is made of a 90 cm length of Teflon tubes coiled on a heat-conducting metal cylinder, and a proportional integral derivative (PID) controller controls the temperature of the reactor at 40–75 °C to accelerate the derivatization reaction. After the derivatization reaction, the sample is sent to the detecting module, which comprises a liquid waveguide capillary cell (LWCC-100, World Precision Instruments, USA) with optical path length of 100 cm, an LED light source with the mode at 665 nm (Ocean Optics) and a phototube (S16008-33, Hamamatsu, Japan) for the long-path photometry detection. The sample solution to be tested is filtered by a 1.0 µm filter before passing through the LWCC to avoid interference from components of the sample matrix or method reagents. Both the fluid propulsion module and the detection module can be computer-controlled.

Equation (5) can help convert the concentration of NH_4^+ solution $C_{NH_4^+}$ to the NH_3 concentration in the gaseous C_{NH_3}.

$$C_{NH_3} = \frac{C_{NH_4^+} F_1 RT}{M_{NH_4^+} F_g P \gamma}, \qquad (5)$$

where C_{NH_3} denotes the content of NH_3 in the air sample (ppb), P denotes atmospheric pressure (101.3 kPa), $M_{NH_4^+}$ denotes the molar mass of NH_3 (18.04 g mol^{-1}) and $R = 8.314$ Pa m^3 mol^{-1} K^{-1}. T denotes the room temperature (K), F_1 denotes the flow rate of stripping solution, F_g denotes the flow rate of sampling gas and γ denotes the capture efficiency of air NH_3 in the stripping solution (a constant determined by laboratory).

2.3 Experiment protocol

The exact recipe of the chemical reactions follows the reactions described by Searle (Searle, 1984). We used 0.75 g L^{-1} salicylic acid (TCI, 99.5 %, Japan), 0.014 g L^{-1} sodium nitroferricyanide (TCI, 99 %, Japan) and 0.2 g L^{-1} NaOH as stripping solution ($R1$) and then the 0.188 mL L^{-1} sodium hypochlorite (Aladdin, active chlorine 10 %, China) and 1.5 g L^{-1} NaOH as derivatization solution ($R2$). We acknowledge that a selective colorimetric reaction to form a highly absorbing reaction product must be carried out under catalytic and alkaline conditions. Sodium nitroferricyanide is recognized as a high-efficiency catalyst to increase the sensitivity of Eq. (4) (Krom, 1980; Searle, 1984).

Calibrating the setup uses NH_4^+ standard solution produced by the National Institute of Metrology, China. The standards are prepared shortly before use by NH_4^+ standard solution with $R1$ in a volumetric bottle for use right after it was ready. The ideal use cycle of $R1$ and $R2$ was half a month; after replacement with new $R1$ and $R2$ solutions and other instrument fittings, the instrument should be recalibrated to ensure data quality.

2.4 Sampling method

The inter-comparison experiment was conducted at the College of Environment Sciences and Engineering, Peking University, located within the 4th Ring Road in northern Beijing, China (39.59° N, 116.18° E). A commercial Picarro G2103 analyzer (Picarro, USA) used for atmospheric NH_3 measurement based on the CRDS method was deployed concurrently with SAC-LOPAP in the comparison, which could be used to validate other instruments (Twigg et al., 2022). The experiment took place from 15 September 2021 to 15 October 2021, with the instruments installed in a field container. Two instruments shared an inlet and were deployed 2.5 m above the ground. A polytetrafluoroethylene (PTFE) filter (46.2 mm diameter, 2 µm pore size, Whatman, USA) is used in the front of the sample module to remove ambient
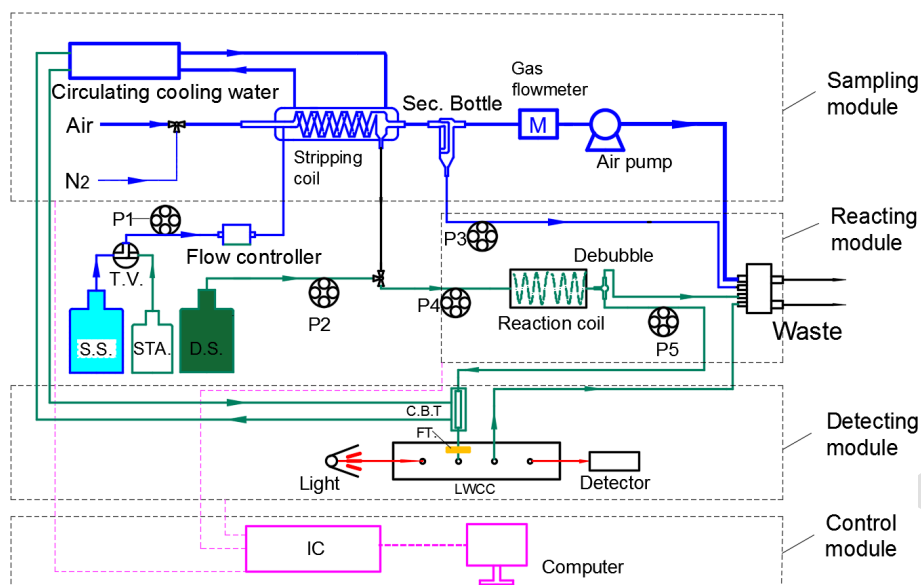
Figure 1. Schematic diagram of SAC-LOPAP. M: gas flowmeter; S.S.: stripping solution; STA.: standard solution; D.S.: derivatization solution; Sec. Bottle: security bottle; C.B.T: cooling buffer tube; T.V.: triple valve for switching stripping solution and standard solution; P1, P2, P3, P4, P5: peristaltic pump for transferring solutions; FT: syringe filter; IC: integrated circuit. The gas flow rate can be controlled from 0.2–$2.0\,\mathrm{L\,min^{-1}}$, with an optimal gas flow rate of $0.7\,\mathrm{L\,min^{-1}}$. The liquid flow rate can be controlled from 0.1–$1.0\,\mathrm{mL\,min^{-1}}$, with an optimal stripping liquid flow rate of $0.49\,\mathrm{mL\,min^{-1}}$.

aerosols, which is placed into a round filter holder made of perfluoroalkoxy (PFA). We changed the filter every day with the aim of avoiding uncertainties. After the filtration of the aerosols, the sample gas flow is delivered into a 3.8 m long 1/4 in. Teflon tube, and a temperature-controlled metal heating wire (set at $35\,°\mathrm{C} \pm 0.1\,°\mathrm{C}$) is wrapped around the sample tube and covered with thermo-isolation materials. We ran our instrument with an additional drag flow of $1.75\,\mathrm{L\,min^{-1}}$ with the aim of ensuring the ambient residence time was about 7.8 ms for all instruments. Data acquisition times were different for the above instruments during the inter-comparison. The base reporting periods for the Picarro and SAC-LOPAP instruments were 1 and 30 s. For the purposes of comparison, data from the two instruments presented in this section were averaged to 30 s. In addition, high-purity N_2 as the zero gas was injected into the sampling tube, carried out every 7 d and at the start and end of the campaign as well. The standard NH_3 source is made by Sichuan Zhongce Biaowu Technology Co., Ltd., from China. The quality management system of the company conforms to the recognized standard in Chinese industry (GB/T9001-2016/ISO 9001:2015). The composition was ammonia (5.08 ppm) and nitrogen, and the uncertainty was 2%. In the test, pure N_2 was used as the dilution gas to obtain the required concentration of ammonia standard gas. Calibrations were performed using combinations of concentrations at 1.32, 4.95, 9.59, 17.90 and 54.96 ppb from the cylinder. In addition, 4.95 and 54.96 ppb standard gas were injected into the sample tube every 7 d after the zero point. The field container was controlled at

$25\,°\mathrm{C} \pm 1\,°\mathrm{C}$ to reduce the impact of temperature fluctuations on measurement results.

3 Characterization and optimization

3.1 Sampling efficiency

NH_3 standard gas of 54.96 ppb was used as the sample to be collected through two identical serial stripping coils, and the concentration of liquid samples collected by the two stripping coils was measured to calculate the capture efficiency. The calculation formula is as below.

$$\gamma_1 = \frac{c_1}{c_1 + c_2} \times 100\%, \tag{6}$$

where γ_1 denotes the collection efficiency of the first stripping coil and c_1 and c_2 denote the concentration of NH_4^+ trapped in the first stripping coil and the second stripping coil, respectively.

The collection efficiency of NH_3 from $R1$ reached more than 99% under different c_{NaOH}, F_1 and F_g conditions. Figure 2a and b show that F_1 and F_g had almost no influence on collection efficiency. Figure 2c shows that a c_{NaOH} of $1.25\,\mathrm{mmol\,L^{-1}}$ achieved the greatest collection efficiency in $R1$ (99.9%). Therefore, the c_{NaOH} of $1.25\,\mathrm{mmol\,L^{-1}}$ was selected as the $R1$ of the NH_3, and we selected F_1 as $0.49\,\mathrm{mL\,min^{-1}}$ and F_g as $0.7\,\mathrm{L\,min^{-1}}$ in order to achieve the required detection range in this study.
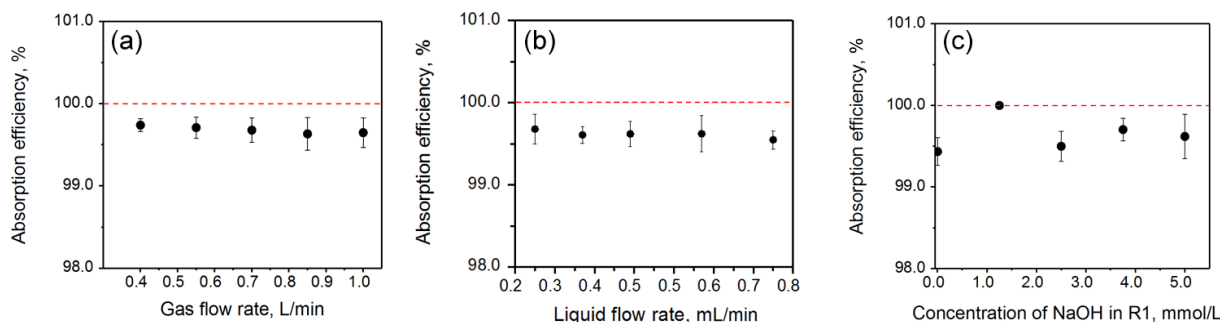
Figure 2. The absorption efficiency of the stripping coil versus the **(a)** gas flow rate ($c_{NaOH} = 4.0 \, \text{mmol L}^{-1}$, $F_l = 0.49 \, \text{mL min}^{-1}$), **(b)** liquid flow rate ($c_{NaOH} = 4.0 \, \text{mmol L}^{-1}$, $F_g = 0.7 \, \text{L min}^{-1}$) and **(c)** concentration of NaOH in $R1$ ($F_l = 0.49 \, \text{mL min}^{-1}$, $F_g = 0.7 \, \text{L min}^{-1}$).

3.2 Setting reaction conditions

Precipitates can attach to the wall of the pipeline and LWCC for online instruments, which leads to pipeline blockage and baseline drift. Therefore, we need to optimize reaction conditions and add the constant-temperature module and liquid flow controller temperature to achieve continuous online measurement of low-concentration ammonia in ambient air. The concentration of the $R1$ we used in the initial reaction conditions (longer optical path and smaller sampling volume) contained $1 \, \text{g L}^{-1}$ salicylic acid, $0.1 \, \text{g L}^{-1}$ sodium nitroprusside and $1 \, \text{g L}^{-1}$ NaOH. A total of $0.5 \, \text{mL L}^{-1}$ of sodium hypochlorite and $3 \, \text{g L}^{-1}$ of NaOH were used as $R2$ (Krom, 1980; Searle, 1984). In addition, the syringe filter was introduced to minimize the influence of precipitate (Bianchi et al., 2012), but a large drift of the baseline would still occur during the long time run in our experiment, which will be discussed in detail later. In fact, we tried interrupting the sampling for a few minutes and implementing 5% hydrochloric acid for the system to remove these precipitates. However, the concentration changed greatly before and after each cleaning precipitation. In addition, once the precipitation is formed, it takes a long time to remove it, which also increases the risk of contaminating the detector. According to reaction kinetics, reducing the stripping and derivatization concentrations (solution concentration) and $[OH^-]$ of the system can greatly reduce the formation of precipitates in the solution. Therefore, we need to find the optimal reaction conditions to produce the least amount of precipitate. The maximum absorbance of a $100 \, \mu\text{g L}^{-1}$ NH_4^+ standard solution was obtained at $18.75 \, \text{mmol L}^{-1}$ OH^-, and we could obtain a high absorbance of light and a slow speed of precipitate formation, which meant that $1.5 \, \text{g L}^{-1}$ NaOH was added to the derivatization solution, resulting in the precipitate in the solution being too small to cause pipeline blockage and baseline drift. Importantly, we added regular assessment of the system drift through use of online sampling of pure N_2. The ranges of blank signal in continuous operation for 48 h were 2.856–2.848 and 2.254–1.834 V of reduced solution concentration and formerly high solution concentra-
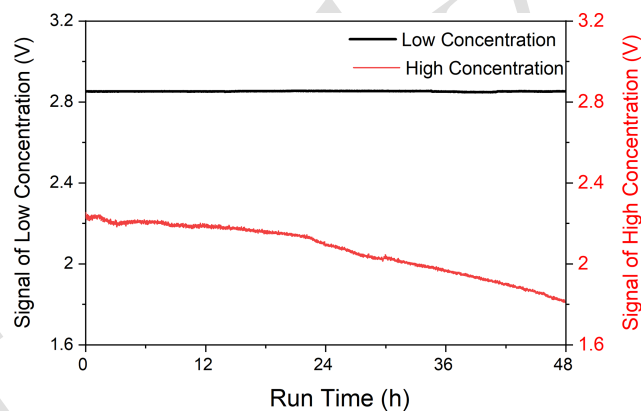
Figure 3. The blank time series of the NH_3 detector ran continuously for 48 h (low concentration: $0.75 \, \text{g L}^{-1}$ salicylic acid, $0.014 \, \text{g L}^{-1}$ sodium nitroferricyanide and $0.2 \, \text{g L}^{-1}$ NaOH as $R1$, then $0.188 \, \text{mL L}^{-1}$ sodium hypochlorite and $1.5 \, \text{g L}^{-1}$ NaOH as $R2$; high concentration: $1 \, \text{g L}^{-1}$ salicylic acid, $0.1 \, \text{g L}^{-1}$ sodium nitroferricyanide and $1 \, \text{g L}^{-1}$ NaOH as $R1$, then $0.5 \, \text{mL L}^{-1}$ sodium hypochlorite and $3 \, \text{g L}^{-1}$ NaOH as $R2$).

tion, and the maximum offset were 0.3% and 18.6%, respectively; the baseline of low-concentration solution has better stability (Fig. 3). In addition, the concentrations of salicylic acid, sodium nitroferricyanide and sodium hypochlorite were 0.04, 0.02 and 0.006 times lower, respectively, than those in previous research (Bianchi et al., 2012). In general, the iron-containing precipitate increases the absorbance by scattering or absorbing light, resulting in measurement bias. In this study, the amount of iron-containing precipitation is very small due to reducing the content of components and alkali of the solution system, and the voltage of the instrument will not drop significantly due to contamination, which is conducive to better maintenance of the baseline.

## 3.3 Stability of liquid flow and temperature

The temperature control module and flow control system were designed because of the sensitivity of molecular absorption spectrophotometry to ambient temperature and res-

idence time. A commercial PID temperature controller was used to control the temperature of the reaction coil with an accuracy of $\pm 0.1\,°C$. The temperature control module was used to control the constant temperature from the reaction coil to the LWCC at $55.0 \pm 0.1\,°C$. At the same time, the flow control system could control the rotational speed of the peristaltic pump. This system used a commercial liquid flowmeter (SLI-1000, Sensirion, Switzerland) to detect the flow rate and feedback to the peristaltic pump control by detecting the flow of tiny bubbles, which further improved the stability of the reaction process. In other words, the flow control system could avoid the flow rate dropping caused by abrasion of the pump tube and increase the flow rate caused by the replacement of the pump tube, keeping the $R1$ flow at a constant set point ($0.49\,mL\,min^{-1}$).

In addition, we designed a buffer tube with a cooling function to further reduce the effects of precipitation. After the derivatization reaction in the reaction coil at $55.0\,°C$, the mixed solution entered the cooling buffer tube. Most of the precipitation was generated in the buffer tube and attached to the tube wall, while some of the precipitation generated in the downstream pipeline was intercepted by an in-line precipitate filter with a pore size of $1.0\,\mu m$ before the LWCC, and the filter was changed weekly.

Overall, the above work can make the instrument maintain a relatively stable reaction time and temperature, which can promote a relatively stable reaction process, resulting in a high reproducibility of the same concentration of NH_3. In the calibration process, $R1$ was used as a diluent, and the concentrations were 10, 25, 50, 75, 100, 150 and $200\,\mu g\,L^{-1}$ of NH_4^+ standard solution. High-purity N_2 was used as a blank gas in the sampling tube, and the standard solution instead of $R1$ entered the solution system. Figure 4 shows the calibration with NH_4^+ concentration gradients of 0, 10, 25, 50 and $100\,\mu g\,L^{-1}$ (150 and $200\,\mu g\,L^{-1}$ of NH_4^+ standard solutions were out of the detection range, which is discussed in Sect. 3.4). Each concentration point was run for 40 min, and the relative standard deviation (RSD) calculated from four consecutive measurements (the collection of the four replicates were completed during 4 weeks of constant instrument operation) ranged from $0.32\,\%$ to $2.65\,\%$, with k varying from 0.0037 to 0.0040. Moreover, the blank experiment tests were automatically made every 1 or 2 d; that is, high-purity N_2 was used as a blank gas through the sample tube for 40 min. The RSD of the blank signal in continuous operation for 1 month was $1.8\,\%$, which indicated good repeatability and stability of the instrument. Seven switching samples were performed with $50\,\mu g\,L^{-1}$ NH_4^+ standard solution and $R1$; after calculating $10\,\%$–$90\,\%$ of the full signal after a change in concentration, the time response was approximately 140 s, which was much quicker than the method described by Bianchi et al. (2012; measured to be 10 min).
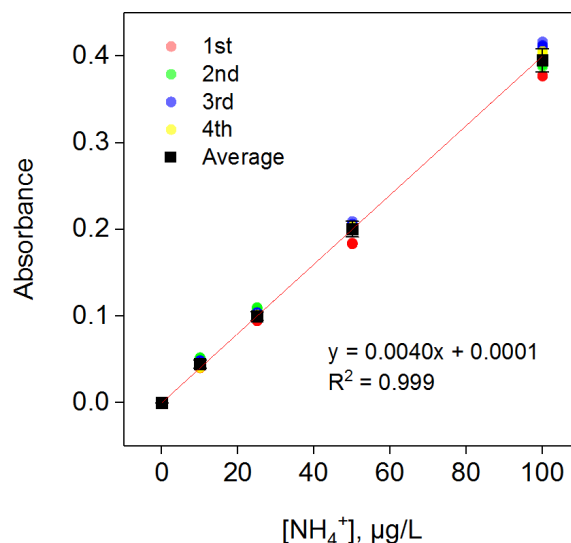

Figure 4. Calibration curves of standard solution with the same concentration gradient four times.

Table 1. Linear regression with the same concentration gradient four times.

Time	k	b	R^2
First	0.0037	0.0018	0.9998
Second	0.0039	0.0046	0.9996
Third	0.0040	0.0034	0.9997
Fourth	0.0040	0.0003	0.9999

3.4 Setup of the temperature

High temperature can accelerate the reaction process and achieve better measurement accuracy and precision. The voltage signal decreased with increasing temperature; conversely, the absorbance increased with temperature. According to the flow rate (gas flow rate of $0.70\,L\,min^{-1}$, liquid flow rate of $0.49\,mL\,min^{-1}$), the detection limit of our SAC-LOPAP can reduce to less than 50 ppt when the absorbance of $50\,\mu g\,L^{-1}$ NH_4^+ standard solution reaches 0.15 or more. However, if the temperature is too high, there is a danger that the pipeline interface of the instrument will fall off. Considering the continuous delivery of solutions (the stability of pipeline connections) and the detection limit (lower than 50 ppt), $55\,°C$ was selected as the best reaction operating temperature of the instrument, at which sufficient absorbance can be achieved to detect concentrations of ammonia gas. The standard solution instead of the stripping solution entered the solution system; then the measured absorbance values were used for absorbance-standard solution concentration plotting and regression calculation. (The experimental process has been described in Sect. 3.3.) The result is shown in Fig. 5: a high degree of correlation was found between the standard solution and absorbance with a correla-
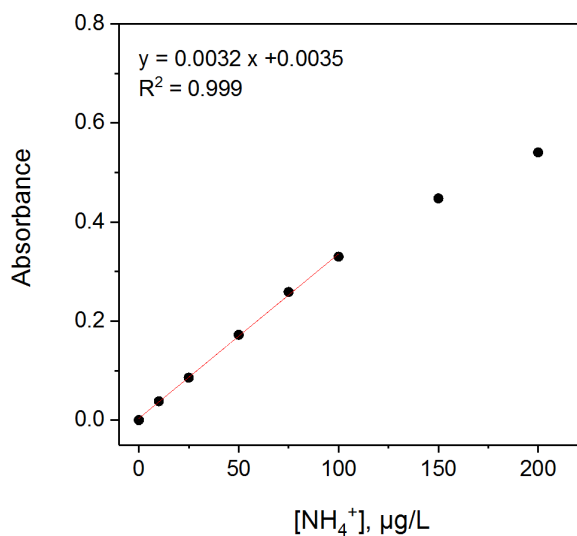
Figure 5. Standard solution and absorbance liner range test to obtain a measurement range.

tion coefficient of $R^2 = 0.99$ for the standard solution of 0–100 µg L^{-1}; however, due to the incomplete reaction of NH$_4^+$ with dye products, there are two points outside of the linear fit (standard solution concentrations are 150 and 200 µg L^{-1}). Therefore, the approximate mixing ratio of NH$_3$ corresponding to the standard liquid concentration is 0–99.1 ppb, which is more than adequate for monitoring urban areas. The detection limit for NH$_4^+$ liquid solution is about 40.9 ng L^{-1}, which is calculated as 3 times the average standard deviation of blank signal noise in 1 h. With an air sample flow rate of 0.7 L min^{-1} and a liquid flow rate of 0.49 mL min^{-1}, this translates to a gas-phase mixing ratio of about 40.5 ppt. In other words, the measurement range was 40.5 up to 99.1 ppb for NH$_3$, which was well suited for the investigation of the NH$_3$ budget for urban to rural conditions in China. At the same time, according to the zero-point data and the calibration, the concentration corresponding to the voltage signal of 0.1 mV is 3.1 ppt, which by far meets our requirements for actual environmental measurement. Importantly, the detection limit can be decreased by improving the gas flow. We can increase our detection range by reducing the reaction temperature and shortening the length of the LWCC. For example, Table 2 could be obtained according to Eq. (5) and the stability ranges of F_l and F_g. The detection limit can be reduced to 14.47 ppt, and the detection upper limit can be increased to 519.02 ppb by adjusting F_l and F_g (Table 2).

4 Comparison in urban Beijing

The time series of the concentration of NH$_3$ during the intercomparison period of Picarro and SAC-LOPAP are presented in Fig. 6a. There were a few data gaps for the above instruments caused by calibration operations and instrument maintenance. Instruments display similar temporal features for NH$_3$ concentrations over the duration of the study. In this study, the concentration of our instrument ranged from 1.3 to 47.86 ppb with an average of 12.64 ± 8.63 ppb, which was close to the concentrations of Picarro (12.76 ± 8.57 ppb). The response speed was similar, indicating that SAC-LOPAP responded in time to rapid changes in NH$_3$ concentration. The diurnal-variation results showed that the concentrations measured by the two instruments were very similar, with our instrument slightly lower than the Picarro one by 0.72 ppb (Fig. 6b). Furthermore, relatively good correlations for the NH$_3$ data observed by these instruments were achieved over a large dynamic range of concentration with a slope of 1.00 and an R^2 of 0.96 (Fig. 6c). We found that most of the time there were good correlations between the two instruments within 1 d except for the data of 23 and 30 September. The regression slope for all the days with higher and lower slopes are 1.46 and 0.72, respectively. We performed in situ testing of both systems with a cylinder, and we produced NH$_3$ concentrations of about 1.32, 4.95, 9.59, 17.90 and 54.96 ppb. Figure 6d shows regression analyses of the NH$_3$ standard gas concentrations obtained with the two instruments. The NH$_3$ concentrations measured by the Picarro instrument and our instrument were strongly correlated, with a slope of 1.01 and an R^2 of 0.99.

In general, our instrument ran relatively stably with the standard deviation of zero gas during the 1 month of observations being within 26 ppt (Picarro: 23 ppt), which was far below our detection limit. Furthermore, the drifts of the SAC-LOPAP and Picarro instruments at 4.95 ppb were 3.5 % and 2.8 %, while the drifts at 54.96 ppb were 1.5 % and 0.7 %, which meant that our instrument could keep steady for a long time and it could be used for the continuous online measurement of low concentration of ambient air. More detailed inter-comparison for these NH$_3$ instruments will be analyzed in a future publication.

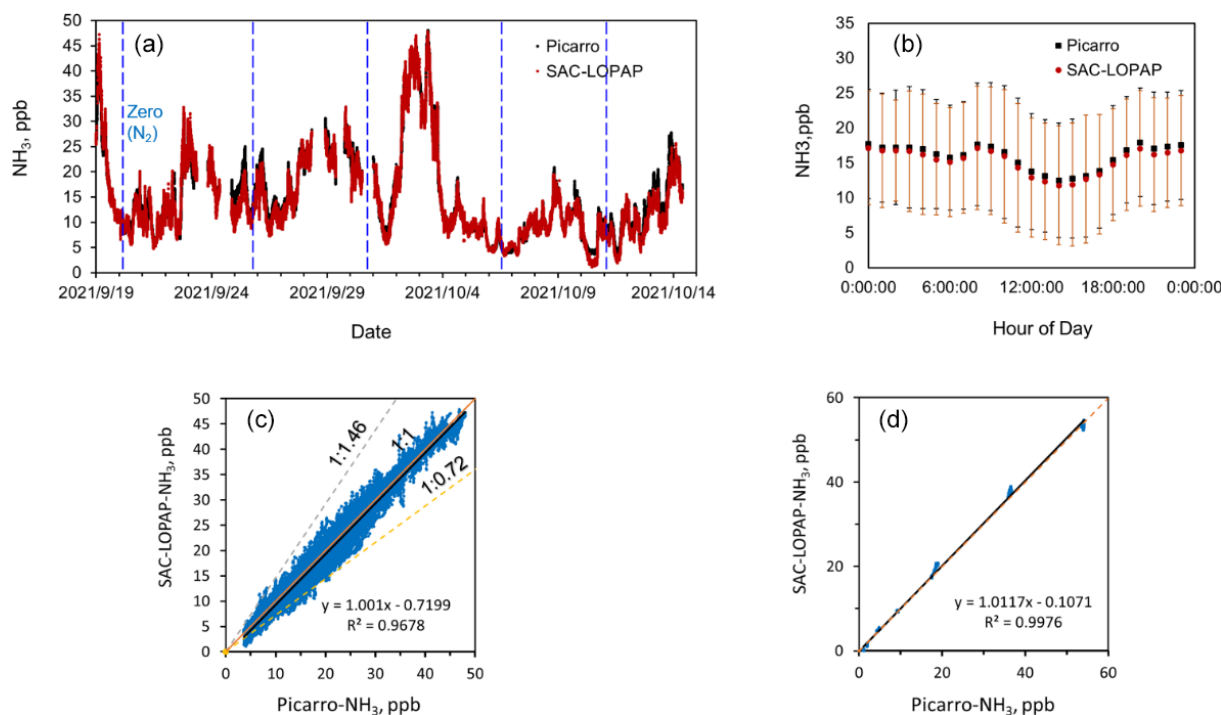## 5 Conclusions

Ammonia (NH$_3$) in the atmosphere affects the environment and human health and is therefore increasingly recognized by policymakers as an important air pollutant that needs to be mitigated. The accurate and precise detection of ambient NH$_3$ concentrations is therefore urgently needed for the exploration of secondary pollution at the regional scale in China.

At the present stage, ambient NH$_3$ measurements at many supersites are still made with spectroscopic, mass spectrometric and wet chemical methods, which are restricted by the high detection limits and lower time resolutions. In this study, we provide an online NH$_3$ monitoring system based on wet-chemistry stripping and a long-path absorption photometer of atmospheric NH$_3$. Our new SAC-LOPAP system has several significant improvements: one is the optimization

Table 2. Relationship between F_l, F_g and detection range of SAC-LOPAP.

F_l, mL min^{-1}	F_g, L min^{-1}	$C(\mathrm{NH_3})_{\min}$, ppt, $[\mathrm{NH_4^+}] = 40.9$ ng L^{-1}	$C(\mathrm{NH_3})_{\max}$, ppb, $[\mathrm{NH_4^+}] = 100$ µg L^{-1}
0.25	1	14.47	35.38
0.35	0.85	23.84	58.29
0.5	0.7	41.35	101.11
0.75	0.4	108.55	265.41
1.1	0.3	212.28	519.02

Figure 6. (a) Time series of NH$_3$ concentration during the comparison (the date format is year/month/day). **(b)** Diurnal variation in NH$_3$ concentrations observed by Picarro and SAC-LOPAP (time is local time). **(c)** Regression analysis of the NH$_3$ concentrations observed by the Picarro and SAC-LOPAP instruments. **(d)** Regression analysis of different concentrations of Picarro and SAC-LOPAP NH$_3$ standard gases.

of reaction conditions. The low concentration but higher flow rate of solutions decreases the precipitate's production, and the cooling buffer tube and the filter trap most of the precipitates. Other improvements are the constant-temperature module and liquid flow controller. The constant-temperature module in the system reduces the influence of ambient temperature on the reaction process and color degree. Similarly, adding a liquid flow controller is helpful to the stability of the flow rate and further increases the stability of the reaction process. These improvements reduce the system error and significantly increase the sustainability of SAC-LOPAP operation. Our instrument reached a detection limit of about 40.5 ppt with a stripping liquid flow rate of 0.49 mL min^{-1} and a gas sample flow rate of 0.70 L min^{-1} in its current condition, and the measuring range of the instrument is 40.5 ppt to 99.1 ppb. Our system has also been characterized in a labo-

ratory setting where we can measure low concentrations. The SAC-LOPAP and Picarro instruments were compared in urban areas for a month with relatively good agreement ($R^2 = 0.967$). In addition, the diurnal-variation results showed that the concentrations of the two instruments were very similar. Therefore, we conclude that our update of the ammonia measurement experimental framework has been successful. However, more research about field measurement and comparison is needed to verify the equipment's performance in routine observation, and the influence of particulate ammonium on the results of NH$_3$ detection also requires further study.

References

Beniwal, A. and Sunny: Electrospun SnO_2/PPy nanocomposite for ultra-low ammonia concentration detection at room temperature, Sensor. Actuat. B, 296, 126660, https://doi.org/10.1016/j.snb.2019.126660, 2019.

Bae, M. S., Demerjian, K. L., Schwab, J. J., Weimer, S., Hou, J., Zhou, X., Rhoads, K., and Orsini, D.: Intercomparison of Real Time Ammonium Measurements at Urban and Rural Locations in New York, Aerosol Sci. Technol., 41, 329–341, https://doi.org/10.1080/02786820701199710, 2007.

Behera, S. N., Sharma, M., Aneja, V. P., and Balasubramanian, R.: Ammonia in the atmosphere: a review on emission sources, atmospheric chemistry and deposition on terrestrial bodies, Environ. Sci. Pollut. Res. Int., 20, 8092–8131, https://doi.org/10.1007/s11356-013-2051-9, 2013.

Benson, D. R., Markovich, A., Al-Refai, M., and Lee, S.-H.: A Chemical Ionization Mass Spectrometer for ambient measurements of Ammonia, Atmos. Meas. Tech., 3, 1075–1087, https://doi.org/10.5194/amt-3-1075-2010, 2010.

Berden, G., Peeters, R., Meijer, G., and Apituley, A.: Open-path trace gas detection of ammonia based on cavity-enhanced absorption spectroscopy, Applied Physics B, 71, 231–216, https://doi.org/10.1007/s003400000302, 2000.

Bianchi, F., Dommen, J., Mathot, S., and Baltensperger, U.: On-line determination of ammonia at low pptv mixing ratios in the CLOUD chamber, Atmos. Meas. Tech., 5, 1719–1725, https://doi.org/10.5194/amt-5-1719-2012, 2012.

Bu, X., Xie, Z., Liu, J., Wei, L., and Ren, H.: Global $PM_{2.5}$-attributable health burden from 1990 to 2017: estimates from the Global Burden of Disease Study 2017, Environ. Res., 197, 111123, https://10.1016/j.envres.2021.111123, 2021.

Callahan, M. R., Rose, J. B., and Byrne, R. H.: Long path-length absorbance spectroscopy: trace copper analysis using a 4.4 m liquid core waveguide, Talanta, 58, 891–898, https://doi.org/10.1016/S0039-9140(02)00403-4, 2002.

Chen, X., Oro, Y., Tanaka, K., Takenaka, N., and Bandow, H.: A New Method for Atmospheric Nitrogen Dioxide Measurements Using the Combination of a Stripping Coil and Fluorescence Detection, Analytical Sciences the International Journal of the Japan Society for Analytical Chemistry, 20, 1019–1023, https://doi.org/10.2116/analsci.20.1019, 2004.

Dong, H.-B., Zeng, L.-M., Hu, M., Wu, Y.-S., Zhang, Y.-H., Slanina, J., Zheng, M., Wang, Z.-F., and Jansen, R.: Technical Note: The application of an improved gas and aerosol collector for ambient air pollutants in China, Atmos. Chem. Phys., 12, 10519–10533, https://doi.org/10.5194/acp-12-10519-2012, 2012.

Fowler, D., Steadman, C. E., Stevenson, D., Coyle, M., Rees, R. M., Skiba, U. M., Sutton, M. A., Cape, J. N., Dore, A. J., Vieno, M., Simpson, D., Zaehle, S., Stocker, B. D., Rinaldi, M., Facchini, M. C., Flechard, C. R., Nemitz, E., Twigg, M., Erisman, J. W., Butterbach-Bahl, K., and Galloway, J. N.: Effects of global change during the 21st century on the nitrogen cycle, Atmos. Chem. Phys., 15, 13849–13893, https://doi.org/10.5194/acp-15-13849-2015, 2015.

Gao, X., Koutrakis, P., Coull, B., Lin, X., Vokonas, P., Schwartz, J., and Baccarelli, A. A.: Short-term exposure to $PM_{2.5}$ components and renal health: Findings from the Veterans Affairs Normative Aging Study, J. Hazard. Mater., 420, 126557, https://doi.org/10.1016/j.jhazmat.2021.126557, 2021.

Gong, D., Liucheng, L. I., Baozeng, L. I., Liping, D., Wang, Y., Yanhua, M. A., Zhang, Z., and Jin, Y.: NH_3 measurement based on cavity enhanced absorption spectroscopy, Laser Technology, 5, 664–668, https://doi.org/10.7510/jgjs.issn.1001-3806.2017.05.009, 2017.

Heland, J., Kleffmann, J., Kurtenbach, R., and Wiesen, P.: A new instrument to measure gaseous nitrous acid (HONO) in the atmosphere, Environ. Sci. Technol., 35, 3207–3212, 2001.

Ianniello, A., Spataro, F., Esposito, G., Allegrini, I., Hu, M., and Zhu, T.: Chemical characteristics of inorganic ammonium salts in $PM_{2.5}$ in the atmosphere of Beijing (China), Atmos. Chem. Phys., 11, 10803–10822, https://doi.org/10.5194/acp-11-10803-2011, 2011.

Janson, R., Rosman, K., Karlsson, A., and Hansson, H.-C.: Biogenic emissions and gaseous precursors to forest aerosols, Tellus, 53, 423–440, https://doi.org/10.1034/j.1600-0889.2001.d01-30.x, 2010.

Khlystov, A., Wyers, G. P., Brink, H., and Slanina, J.: The steam-jet aerosol collector (SJAC), J. Aerosol Sci., 26, S111–S112, https://doi.org/10.1016/0021-8502(95)96963-8, 1995.

Kleffmann, J., Heland, J., Kurtenbach, R., Lrzer, J. C., and Wiesen, P.: A new instrument (LOPAP) for the detection of nitrous acid (HONO), Environ. Sci. Pollut. R., 9, 48–54, 2002.

Klimczyk, M., Siczek, A., and Schimmelpfennig, L.: Improving the efficiency of urea-based fertilization leading to reduction in ammonia emission, Sci. Total Environ., 771, 145483, https://doi.org/10.1016/j.scitotenv.2021.145483, 2021.

Krom, M. D.: Spectrophotometric determination of ammonia: a study of a modified Berthelot reaction using salicylate and dichloroisocyanurate, Analyst, 105, 305–316, https://doi.org/10.1039/an9800500305, 1980.

Krupa, S. V.: Effects of atmospheric ammonia (NH_3) on terrestrial vegetation: a review, Environ. Pollut., 124, 179–221, https://doi.org/10.1016/S0269-7491(02)00434-7, 2003.

Makkonen, U., Virkkula, A., Mäntykenttä, J., Hakola, H., Keronen, P., Vakkari, V., and Aalto, P. P.: Semi-continuous gas and inorganic aerosol measurements at a Finnish urban site: comparisons with filters, nitrogen in aerosol and gas phases, and aerosol acidity, Atmos. Chem. Phys., 12, 5617–5631, https://doi.org/10.5194/acp-12-5617-2012, 2012.

Martin, N. A., Ferracci, V., Cassidy, N., and Hoffnagle, J. A.: The application of a cavity ring-down spectrometer to measurements of ambient ammonia using traceable primary standard gas mixtures, Applied Physics B, 122, 219, https://doi.org/10.1007/s00340-016-6486-9, 2016.

Mcmanus, J. B., Nelson, D. D., Shorter, J. H., Zahniser, M. S., and Faist, J.: Quantum cascade lasers for open- and closed-path measurement of trace gases, in: Society of Photo-Optical Instrumentation Engineers (SPIE) Conference Series, Seattle, WA, United States, September 2002, 4817, https://doi.org/10.1117/12.452093, 2002.

Ni, J.-Q., Heber, A. J., Lim, T. T., Diehl, C. A., Duggirala, R. K., Haymore, B. L., and Sutton, A. L.: Ammonia Emission from a Large Mechanically-Ventilated Swine Building during Warm Weather, Journal of Environment Quality, 29, 751–751, https://doi.org/10.2134/jeq2000.00472425002900030010x, 2000.

Nowak, J. B., Neuman, J. A., Kozai, K., Huey, L. G., Tanner, D. J., Holloway, J. S., Ryerson, T. B., Frost, G. J., McKeen, S. A., and Fehsenfeld, F. C.: A chemical ionization mass spectrometry technique for airborne measurements of ammonia, J. Geophys. Res.-Atmos., 112, D10S02, https://doi.org/10.1029/2006jd007589, 2007.

Qu, Z. C., Li, B. C., and Han, Y. L.: Cavity ring-down spectroscopy for trace ammonia detection, J. Infrared Millim. W., 31, 431–436, 2012.

Searle, P. L.: The berthelot or indophenol reaction and its use in the analytical chemistry of nitrogen. A review, Analyst, 109, 549–540, https://doi.org/10.1039/an9840900549, 1984.

Sharma, S. K., Datta, A., Saud, T., Saxena, M., Mandal, T. K., Ahammed, Y. N., and Arya, B. C.: Seasonal variability of ambient NH_3, NO, NO_2 and SO_2 over Delhi, J. Environ. Sci., 22, 1023–1028, https://doi.org/10.1016/S1001-0742(09)60213-8, 2010.

Sharma, S. K., Singh, A. K., Saud, T., Mandal, T. K., Saxena, M., Singh, S., Ghosh, S. K., and Raha, S.: Measurement of ambient NH_3 over Bay of Bengal during W_ICARB Campaign, Ann. Geophys., 30, 371–377, https://doi.org/10.5194/angeo-30-371-2012, 2012.

Sutton, M. A., Fowler, D., Burkhardt, J. K., and Milford, C.: Vegetation atmosphere exchange of ammonia: canopy cycling and the impacts of elevated nitrogen inputs, Water Air Soil Poll. 85, 2057–2063, https://doi.org/10.1007/BF01186137, 1995.

Swati, A. and Hait, S.: Greenhouse Gas Emission During Composting and Vermicomposting of Organic Wastes – A Review, Clean-Soil Air Water, 46, 1700042, https://doi.org/10.1002/clen.201700042, 2018.

Twigg, M. M., Berkhout, A. J. C., Cowan, N., Crunaire, S., Dammers, E., Ebert, V., Gaudion, V., Haaima, M., Häni, C., John, L., Jones, M. R., Kamps, B., Kentisbeer, J., Kupper, T., Leeson, S. R., Leuenberger, D., Lüttschwager, N. O. B., Makkonen, U., Martin, N. A., Missler, D., Mounsor, D., Neftel, A., Nelson, C., Nemitz, E., Oudwater, R., Pascale, C., Petit, J.-E., Pogany, A., Redon, N., Sintermann, J., Stephens, A., Sutton, M. A., Tang, Y. S., Zijlmans, R., Braban, C. F., and Niederhauser, B.: Intercomparison of in situ measurements of ambient NH_3: instrument performance and application under field conditions, Atmos. Meas. Tech., 15, 6755–6787, https://doi.org/10.5194/amt-15-6755-2022, 2022.

von Bobrutzki, K., Braban, C. F., Famulari, D., Jones, S. K., Blackall, T., Smith, T. E. L., Blom, M., Coe, H., Gallagher, M., Ghalaieny, M., McGillen, M. R., Percival, C. J., Whitehead, J. D., Ellis, R., Murphy, J., Mohacsi, A., Pogany, A., Junninen, H., Rantanen, S., Sutton, M. A., and Nemitz, E.: Field inter-comparison of eleven atmospheric ammonia measurement techniques, Atmos. Meas. Tech., 3, 91–112, https://doi.org/10.5194/amt-3-91-2010, 2010.

Wang, R., Ye, X., Liu, Y., Li, H., Yang, X., Chen, J., Gao, W., and Yin, Z.: Characteristics of atmospheric ammonia and its relationship with vehicle emissions in a megacity in China, Atmos. Environ., 182, 97–104, https://doi.org/10.1016/j.atmosenv.2018.03.047, 2018.

Wang, Y., Zhang, Q. Q., He, K., Zhang, Q., and Chai, L.: Sulfate-nitrate-ammonium aerosols over China: response to 2000–2015 emission changes of sulfur dioxide, nitrogen oxides, and ammonia, Atmos. Chem. Phys., 13, 2635–2652, https://doi.org/10.5194/acp-13-2635-2013, 2013.

Warneck, P.: Chemistry of the Natural Atmosphere, International geophysics series, Academic Press, San Diego, c1988, 717 pp., https://doi.org/10.1029/89eo00197, 1988.

Wen, L., Xue, L., Wang, X., Xu, C., Chen, T., Yang, L., Wang, T., Zhang, Q., and Wang, W.: Summertime fine particulate nitrate pollution in the North China Plain: increasing trends, formation mechanisms and implications for control policy, Atmos. Chem. Phys., 18, 11261–11275, https://doi.org/10.5194/acp-18-11261-2018, 2018.

Whitehead, J. D., Twigg, M., Famulari, D., Nemitz, E., Sutton, M. A., Gallagher, M. W., and Fowler, D.: Evaluation of Laser Absorption Spectroscope Techniques for Eddy Covariance Flux Measurements of Ammonia, Environ. Sci. Technol., 42, 2041–2046, https://doi.org/10.1021/es071596u, 2008.

Yao, W., Byrne, R. H., and Waterbury, R. D.: Determination of Nanomolar Concentrations of Nitrite and Nitrate in Natural Waters Using Long Path Length Absorbance Spectroscopy, Environ. Sci. Technol., 32, 2646–2649, https://doi.org/10.1021/es9709583, 1998.

Yokelson, R., Christian, T., Bertschi, I., and Hao, W.: Evaluation of adsorption effects on measurements of ammonia,

acetic acid, and methanol, J. Geophys. Res.-Atmos., 108, 4649, https://doi.org/10.1029/2003JD003549, 2003.

Yu, H. and Lee, S. H.: Chemical ionisation mass spectrometry for the measurement of atmospheric amines, Environ. Chem., 9, 190–201, https://doi.org/10.1071/EN12020, 2012.

Remarks from the typesetter

TS1   Please give an explanation of why Eqs. (3) and (4) need to be changed. We have to ask the handling editor for approval. Thanks.

TS2   Please give an explanation of why this needs to be changed. We have to ask the handling editor for approval. Thanks.

TS3   Please confirm the unit.

TS4   Please note: acknowledgements reinserted. Please confirm both acknowledgements and financial support sections.